Surface Clutter Suppression Techniques for Ice Sounding Radars: Analysis of Airborne Data

Rolf Scheiber(1), Pau Prats(1) and Florence Hélière(2)
(1) German Aerospace Center (DLR), Microwaves and Radar Institute, 82234 Oberpfaffenhofen, Germany
(2) European Space Agency (ESA), European Space Research and Technology Centre, 2201 AG Noordwijk, Netherlands

Abstract

For the ice sounding of Antarctica from space, a P-band radar at 435 MHz is the only option which complies with present ITU regulations. At this frequency the ice surface cannot be considered smooth, leading to high ambiguous returns. Besides simulation, data acquired by airborne sensors are used to evaluate algorithms for surface clutter suppression and mitigation possibilities of ionospheric influence. This paper presents first an analysis of sub-surface along track focussing in the presence of azimuth slopes. For across-track clutter suppression the multiple-aperture technique in nadir looking geometry is considered, in a repeat-pass configuration as the most general case. Airborne data acquired by the E-SAR system of DLR during ICESAR 2007 campaign are investigated to address feasibility questions for the spaceborne case.

1 Introduction

One of the main problems to be considered for radar sounding in the airborne geometry but even more essential in the space-borne case is the presence of clutter (off-nadir signal components). It superimposes the nadir signal of interest, which is the reflection of the radar wave from different layers within the subsurface and from the bedrock. In the along-track direction coherent summation of succesive pulses has been performed in the past, but recent research has demonstrated the benefits of fully focused SAR processing [1,2]. Special attention needs to be given to the refraction at the ice surface. In section 2 the sub-surface signal description and matched filter approach adopted in [2] is extended to the case of along track slopes, and conclusions for the air- and spaceborne case are taken.
For the across-track direction different approaches have been proposed recently. The multiple-beam antenna technique [3] can be shown to be a special case of a generalized repeat-pass or multiple phase center approach [5]. Another technique makes use of an interferometer in off-nadir configuration. Its main challenge is the separation of ice surface and bedrock topography interferometric phase contributions [4]. Very recently, also clutter suppression by polarisation diversity has been proposed by K. Raney, a technique which aims to evaluate different polarisation characteristics of the nadir and off-nadir reflections. Section 3 focuses on the multiple phase center approach. First we describe the sounding geometry and the algorithm implementation. The main characteristics of the airborne E-SAR system in P-band are then summarized together with the experiment description which was performed during the ICESAR-2007 campaign on Svalbard. The intention was a first attempt towards the demonstration of the technique with airborne data acquired on multiple parallel tracks. Although the data evaluation was not fully succesfull in this respect, some important conclusions can be taken from the analysis presented in section 5.

2 Along-track focussing in the presence of slopes

The along-track sounder geometry in the presence of azimuth slopes is depicted in Fig. 2. The signal history is evaluated for the center of a data block and a constant azimuth slope α is assumed.

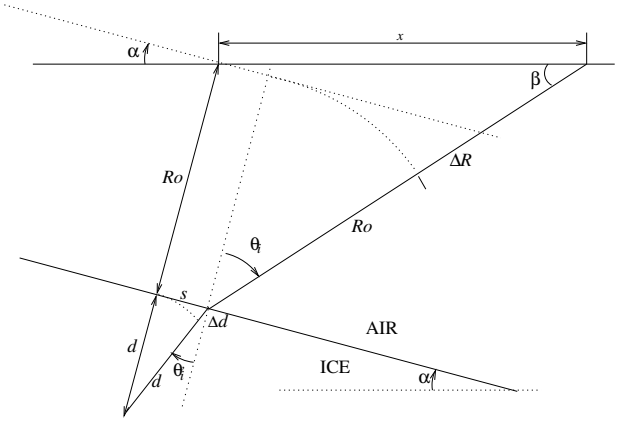

Figure 1: Along track sounder geometry in the presence of azimuth slopes.

Using the law of sines, the incidence angle θ_i as a function of azimuth position x can be evaluated:

$$\begin{aligned} &\sin\theta_i = (x\cos\alpha - s)/\sqrt{N}, \text{ with} \\ &N = x^2 + R_0^2 + s^2 + 2xR_0\sin\alpha - 2xs\cos\alpha \end{aligned} \tag{1}$$

Investigating Snell's law of refraction at the ice surface, it is possible to establish and solve a fourth order polynomial equation for s (see also derivation in [2] for the zero slope case):

$$\begin{aligned} &(\epsilon_r - 1)\cdot s^4 - 2x\cos\alpha(\epsilon_r - 1)\cdot s^3 + \\ &+[(\epsilon_r - \cos^2\alpha)x^2 + \epsilon_r R_0^2 - d^2 + 2xR_0\epsilon_r\sin\alpha]\cdot s^2 + \\ &+2d^2x\cos\alpha\cdot s - d^2x^2\cos^2\alpha = 0. \end{aligned} \tag{2}$$

The sub-surface signal phase, which takes into consideration the refraction at the ice surface, can than be computed as:

$$\phi_{air:ice} = -4\pi/\lambda(\Delta R + \sqrt{\epsilon_r}\Delta d), \tag{3}$$

with:

$$\begin{aligned} &\Delta R = \sqrt{R_1^2 + x_1^2 + 2R_1x_1 sin(\alpha)} - R_0, \\ &R_1 = R_0 + s\tan\alpha, \\ &x_1 = x - s/\cos\alpha. \end{aligned} \tag{4}$$

A comparative analysis with signals propagating from the same closest approach delay, but in free air can now be performed (for this reference case the signal phase is hyperbolic and efficient SAR processing algorithms exist). For airborne geometries it can be shown that, if refraction is not considered, along-track defocussing occurs already for small ice depth of around one hundred meters. In the presence of slopes, an additional azimuth mislocation is encountered, which increases with ice depth.

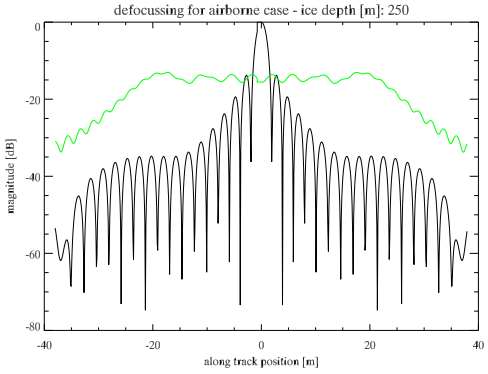

Figure 2: Refraction induced azimuth defocussing (P-band airborne case) for an ice depth of 250m.

An example for the defocussing at an ice depths of 250m is presented in Fig. 2 assuming a P-band sensor at an altitude of 1500m above the ice surface (with resolution of 2m). For larger ice depths the effects of uncompensated range migration must be considered (e.g. via a 2D matched filter as suggested in [1]. The mislocation in azimuth due to a slope of 1 deg is ∼5m for this example and increases to ∼20m for an ice depth of 1000m. For the spaceborne case, the defocussing effect is less severe but should be accounted for for ice depths exceeding one kilometer. The mislocation due to azimuth slopes is very similar to the airborne case.

3 Across-Track Clutter Suppression

As a generalized approach, the across-track clutter suppression method summarized here was first suggested for the repeat-pass case [5] but can also be adapted for a multiple phase center antenna. A short summary is given next.

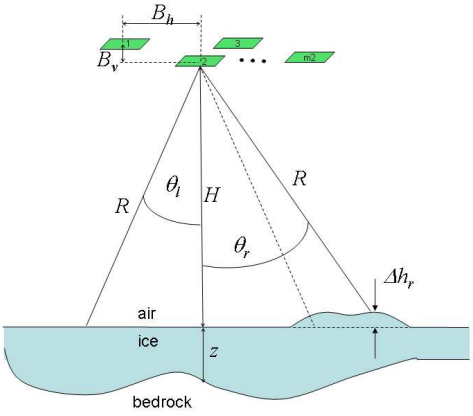

Figure 3: Cross track sounder geometry with repeated acquisitions (general case)

Fig. 3 shows the geometry of a nadir looking radar sounder. The flight direction of the airborne or satellite sensor is into the paper plane. The cross-track surface clutter is superimposing the signal of interest from the nadir direction. Note that due to the terrain topography the geometry is generally not symmetrical. Signals reflected from the left and right of the nadir track are also within the main lobe of the antenna beam. From the knowledge of the geometry, one can compute the directions of surface ambiguity $\theta_{l,r}$ as a function of ice thickness:

$$\theta_{l,r} = \arccos\frac{H - dh_{l,r}}{H + n\cdot z} = \arccos\frac{H - dh_{l,r}}{R}, \tag{5}$$

where H is the height of the antenna above the reference plane, dh_l and dh_r are the elevations of the left and right ambiguities above the reference plane, n is the refractive index of ice and z the ice depth from which information is required.

In a next step the antenna diagram matrix $\mathbf{A}$ is computed and a system of linear equations is set up:

$$\mathbf{A}_{m_1\cdot m_2}\cdot\mathbf{w}_{m_2\cdot 1} = \mathbf{r}_{m_1\cdot 1}. \tag{6}$$

$\mathbf{A}$ is of size m_1 by m_2. m_1 stands for the number of angles of interest (e.g. 3 corresponding to nadir, and to the first left and first right side ambiguity) and m_2 for the number of antennas/acquisitions. $\mathbf{A}$ contains the phasors for the m_1 directions of interest weighted by the antenna patterns

(for $\theta = 0$,$\theta = \theta_r$,$\theta = \theta_l$). Using the parallel ray approximation, the elements of the matrix **A** are given as:

$$a_{k,i}(\theta_i) = G_k(\theta_i) \cdot \exp\left[\frac{j4\pi}{\lambda} \cdot (B_{h,k} \sin\theta_i + B_{v,k} \cos\theta_i) - \phi_{cal,k}\right], \quad (7)$$

where G_k is the complex valued gain for acquisition k and θ_i is the angle of interest. The calibration phase $\phi_{cal,k}$ accounts for different propagation phase offsets (e.g. due to atmospheric and ionospheric effects) and may be estimated independently for each data acquisition k from the phase of the reflection of the air ice interface (i.e. the first strong echo). For multiple phase center antennas usually transmit is performed with the complete aperture and reception is done in parallel for different apertures or their combinations. In this case the antenna gain in eq. 7 must be computed accordingly and the phasors must account for the one way phase difference only. In case multiple beams are formed with co-located phase centers, the baselines become zero and the matrix elements correspond to the gain of the different beams in the different directions. The column vector **r** in eq. 6 contains the information about the desired gain of the constellation. For instance $r[0] \neq 0$ for $\theta = 0$ and $r[i] = 0$ for $\theta = \theta_r$ and $\theta = \theta_l$. This ensures signal cancellation in the directions of the surface clutter θ_r and θ_l and no cancellation in the nadir direction. The linear system in eq. 6 can be solved in case there is a right inverse for the matrix **A** and a figure of merit for the reconstruction is derived by evaluating the resulting adaptive sparse antenna array pattern. Further details can be found in [5].

4 P-band Data Acquisition

Part of the (side-looking) E-SAR sensor is a fully polarimetric P-band sub-system which is operated at a center frequency of 350 MHz with a bandwidth of up to 100 MHz. An additional feeding network has been included in the antenna to allow pointing the antenna in the nadir direction for purposes of P-band ice sounder data acquisition. The antenna provides a single beam 30 deg wide in across track. Unfortunatly, the antenna design did not foresee the separation of the antenna into multiple apertures (phase centers). With this hardware setting two test data sets were acquired during the ICESAR 2007 campaign on Svalbard. The first data set of 3+3 lines has been taken at low altitudes of 1800m above ice surface on March, 25 at the summit area of Nordaustlandet. As the detection of the bedrock was not possible in this area, the second data set was acquired on April, 20 at the glacier area, closer to the margin of the ice sheet, this time at the highest altitude supported by the aircraft, i.e. 4600 m above the ice sheet. This second data set is subject to the analysis presented in this paper. The horizontal baselines flown by the pilots of the Do-228 aircraft carrying the E-SAR system are shown in Fig. 4. Odd and even track-ID refer to opposite flight directions. Unfortunatly, the vertical baselines of half of the data takes is shifted by more than 20m from the others due to a temporary loss of the GPS link. This turned out to be a major problem in the attempt of clutter rejection according to the method in section 3. During ICESAR also side-looking data takes were taken at P-band with different spatial and temporal baselines.

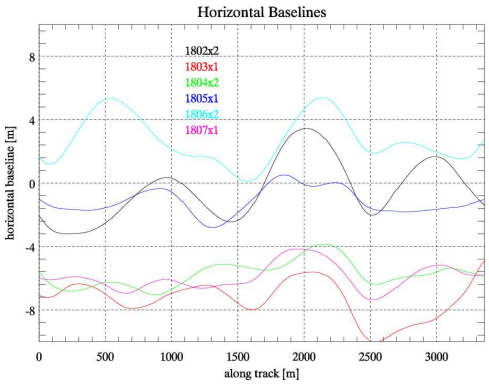

Figure 4: Sounder baselines acquired during the ICESAR campaign (relative to track 1801x1).

5 Data Analysis

5.1 Temporal decorrelation analysis

For the multiple phase center technique the ice volume under investigation and particularly the ice surface is assumed to be correlated, i.e. temporal decorrelation might be an issue for the general case of a repeat-pass scenario as described in section 3. For the investigation of the amount of temporal decorrelation side-looking P-band measurements have been performed during the ICESAR campaign. The temporal separation was in the order of 3 weeks.

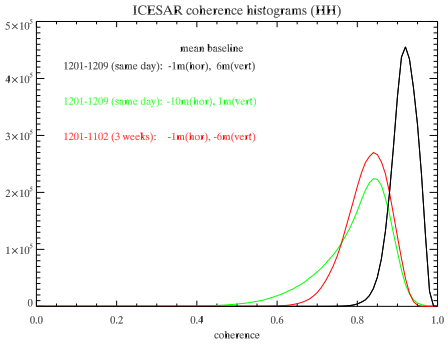

Figure 5: Coherence histograms as indicators for temporal decorrelation.

Fig. 5 presents the coherence histograms in HH polarisation for the Glacier test site. Two different spatial baselines were evaluated with same day flights (negligible temporal baseline, black and green lines) and compared to the three

weeks temporal baseline (red line). The main decorrelation source for the same day coherence is volume decorrelation. This term is also dominating the three weeks coherence (similar baselines), and therefore the amount of temporal decorrelation is anticipated to be quite small. A more precise assessment of temporal decorrelation was not possible as smaller baselines are not available.

5.2 Coherent combination analysis

The first interferometric analysis towards the demonstration of the clutter suppression technique described in section 3 is with respect to the estimation of the calibration phase ϕ_{cal} from the first strong nadir reflection. The estimation of the calibration phase from interferometric combinations of sounder data seems feasible. Note, that this method could be applied to estimate different (azimuth varying) phase offsets induced by ionosphere in a repeat-pass space-borne sounding scenario. Unfortunatly, only for the small horizontal baseline pair (1801 with 1805) the subsurface return was coherent as can be seen in Fig. 6. Due to the lack of further small baselines, the clutter suppression method described in section 3 could not be attempted.

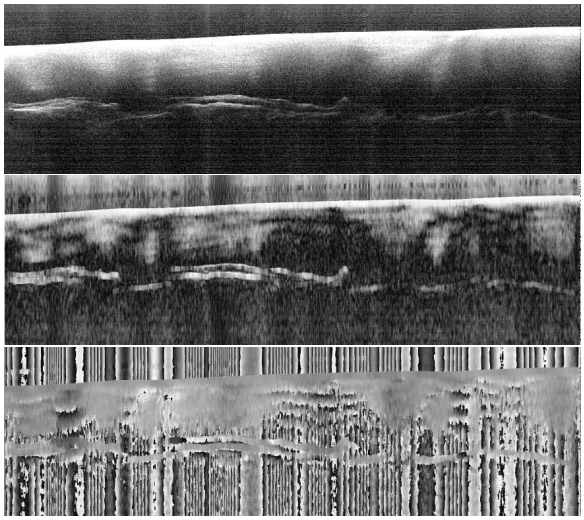

Figure 6: Sounder profile (length: 10km, dynamic range: 30dB) for HV polarisation (top), interferometric coherence (scale 0-1) (middle) and phase (bottom) for the small baseline pair 1801-1805.

Another conclusion is with respect to the sub-surface focussing. Although the E-SAR system was capable to detect the bedrock down to $\sim$570m, we didn't note any improvement/change of subsurface resolution and/or coherence when applying the additional along-track focussing for compensation of refraction at the ice surface. This could be attributed to the flat and homogeneous bedrock and/or to the inhomogeneous ice volume, which does not fit to the assumptions of section 2.

6 Conclusion

In this paper we presented an analysis of the ice sounder signal in the presence of azimuth slopes. In general, the refraction must be accounted for during focused SAR processing of sounder data. For cancellation of across-track clutter a method based on multiple apertures (which may be realised with repeated passes in a general case) was presented. The analysis conducted with airborne data acquired during the ICESAR2007 campaign on Nordaustlandet (Svalbard) allowed first assessment of the described techniques. Unfortunatly, the amount of data is very limited, covering only non-typical scenarios (percolation zone). Nevertheless, new attempts for demonstration are considered for the near future.

7 Acknowledgment

The authors would like to thank the E-SAR team for reconfiguring the P-band antenna to nadir-looking mode and for acquiring the data. This work is supported by ESA contracts no. 19961/06/NL/HE and 20655/07/NL/CB.

References

[1] J.J. Legarsky, S.P. Gogineni, T.L. Akins: *Focused Synthetic Aperture Radar Processing of Ice-Sounder Data Collected over the Greenland Ice Sheet* IEEE Trans. Geosc. Rem. Sens, vol. 39, no. 10, pp. 2109-2117 October, 2001.

[2] F. Hélière, C.C. Lin, H. Corr, D. Vaughn: *Radio Echo Sounding of Pine Island Glacier, West Antarctica: Aperture Synthesis Processing and Analysis of Feasibility from Space* IEEE Trans. Geosc. Rem. Sens, vol. 45, no. 8, pp. 2573-2582 August, 2007.

[3] J. Dall, N. Skou, A. Kusk, S.S. Kristensen, V. Krozer: *Design of an airborne P-band ice sounding radar* Advanced Sensors for Earth Observation; ESA/ESTEC workshop, December, 2006.

[4] E. Rodriguez, A. Freeman, K. Jezek, X. Wu: *A New Technique for Interferometric Sounding of Ice Sheets* EUSAR Proceedings, Dresden, Germany, 2006.

[5] R. Scheiber, P. Prats: *Surface Clutter Suppression for Ice Sounding Radars by Coherent Combination of Repeat-Pass Data* IGARSS Proceedings, Barcelona, Spain, 2007.